Effect of heat treatment on the microstructure and microchemistry of explosive welded joints of Ti-5Ta-1.8Nb and 304L SS

(Winner of **I.T. Mirchandani Memorial Research Award** for best Research Paper in Welding in **NWS 2010**)

C. Sudha*, T.N. Prasanthi, S. Saroja and M. Vijayalakshmi
Physical Metallurgy Division, Metallurgy and Materials Group, Indira Gandhi Center for Atomic Research, Kalpakkam-603 102, Tamilnadu, India
*E-mail : sudha@igcar.gov.in

ABSTRACT

Explosive welding process was used for joining Ti-5Ta-1.8Nb alloy to 304L austenitic stainless steel to avoid the formation of intermetallic phases at the interface which otherwise form in fusion welding processes. Both X-ray diffraction and electron microprobe based analysis showed the absence of intermetallic phases at the weld interface within their detection limits. Strain induced phase transformation due to the deformation induced by explosive welding was observed in both the base materials. The 'as received' explosive joints were further heat treated at 873 and 1073 K for durations in the range of 1 to 20 h to select appropriate temperature for further processing subsequent to welding. Detailed analysis using electron microprobe showed considerable microstructural and micro chemical modification at the weld interface due to inter-diffusion of Fe, Ti, Cr and Ni. The width and number of reaction zones varied as a function of heat treatment temperature and time. From the experiments, it was inferred that even the lowest temperature-time combination, i.e. 873 K-1h, is not suitable for heat treatment of explosive joints of Ti-5Ta-1.8Nb/SS 304L, and further lowering of the process temperature is required.

Keywords: Explosive welding, Ti-5Ta-1.8Nb, 304L stainless steel, heat treatment, intermetallic phases

INTRODUCTION

A Ti based alloy of nominal composition Ti-5Ta-1.8Nb is chosen as the candidate material for the electrolytic dissolver tanks in nuclear fuel reprocessing plants due to its excellent corrosion resistance in boiling nitric acid environment. The electrolytic dissolver tank made of the Ti based alloy has to be joined to the rest of the piping in the plant made of AISI type 304L austenitic stainless steel. Mechanical joints are not suitable since leak tightness is an absolute necessity for such critical application [1]. Conventionally used fusion welding process like TIG welding also cannot be used for joining TiTaNb and 304L stainless steel (SS) due to the formation of intermetallic phases like FeTi and Fe_2Ti which make the weld interface brittle and susceptible for failure during service. Hence, for joining TiTaNb and 304L SS, solid state welding processes are chosen since they do not involve the inter-diffusion of alloying elements and subsequent formation of intermetallic phases if the process parameters are carefully optimized.

Explosive welding is a solid state welding technique which can be successfully used to weld dissimilar systems which cannot be otherwise welded by fusion or diffusion joining methods [2]. During explosion, the base plate and the flier plate get bonded to each other because of the high pressure created near the interface which is much higher than the dynamic yield strength of the material. Due to high pressure waves, metals near the interface undergo severe plastic deformation, and behave like fluids showing frozen flow patterns after welding. It has been reported that during bond zone formation no diffusion occurs due to rapid self quenching of the metals [3]. Brittle intermetallic phases which form as separate zones parallel to the interface in fusion welding processes are completely eliminated or minimized by forming isolated zones surrounded by ductile matrix in explosion welding method.

Explosive welding of cp-titanium to 304 SS has been already demonstrated through optimization of the process parameters to get intermetallic free interface [4]. Hence, in the present work, Ti-5Ta-1.8Nb alloy and SS 304L are welded using explosive welding technique, and the nature of the bond interface is studied. Explosion welded joints are normally stress relieved at 823-923 K in order to remove the effect of cold work from the bond zone [5] or annealed at high temperature [6] before hot rolling to achieve the final dimensions. Heat treatment is expected to promote diffusion of alloying elements leading to the formation of intermetallic phases. Since process temperature plays an important role in the formation of intermetallic phases, an attempt is made in this work to understand the changes in the interface microstructure and microchemistry of explosive cladded joints of TiTaNb and 304L SS after heat treatment.

EXPERIMENTAL DETAILS

Chemical composition and mechanical test results of 304L stainless steel and TiTaNb alloy used in the present work are given as Table 1 and Table 2 respectively.

Ti-5Ta-1.8Nb plate of dimension 250 x 450 x 6 mm was welded to 304L SS plate of dimension 250 x 400 x 6 mm using explosive welding technique patented by M/s Gulf Oil Corporation, Roorkela. Due to mechanical property consideration, TiTaNb and 304L SS were chosen as overlay and base plates respectively. After welding, the plate was cut into smaller specimens of equal dimension. The specimens were sealed in evacuated quartz tubes and heat treated at temperature of 873 and 1073 K for time duration in the range of 1 to 20 h followed by furnace cooling. Cross section of 'as received' and heat treated joints were then metallographically prepared to a mirror finish using silicon carbide papers and 0.1 μm alumina paste. Then the specimens were etched selectively using Kroll's reagent on TiTaNb side and equal amount of $HCl+HNO_3$+distilled water on 304L SS side to reveal the microstructure.

Microstructural examination of 'as received' and heat treated welds was carried out using an optical microscope (MEF4A of M/s Leica) and scanning electron microscope (XL 30 ESEM of M/s FEI, The Netherlands) which was attached with an energy dispersive spectrometer (EDS). Leitz micro-hardness tester with an applied load of 100 g was used for microhardness measurements. X-ray diffractometer (XRG3000 model of M/s INEL) equipped with a curved position sensitive detector was used to identify different phases formed at the interface as well as in overlay and base plates. Cu Kμ was used as the incident radiation at 40 kV and 30 mA. Angular 2θ range from 10° to 90° was covered with a step size of 0.012°.

Table 3
Details of the analyzing crystals used for elemental analysis

Analyzing crystal	Element detected	X-ray reflection used to quantity
LiF	Fe, Cr, Ni, Mn	Kμ
PET	Ti Nb	Kμ Lμ
TAP	Si Ta	Kμ Mμ

Table 1 Chemical composition and mechanical property of 304L stainless steel

Element	C	Si	Mn	P	S	Cr	Ni	N	Fe
wt%	0.02	0.57	1.66	0.029	0.004	18.15	8.59	0.031	Balance
Yield strength (YS)			-	280 N/mm^2					
Ultimate Tensile Strength (UTS)			-	566 N/ mm^2					
%Elongation (L_o = 50 mm)			-	62					

Table 2 Chemical composition and mechanical property of TiTaNb alloy

Element	C	N	H	Fe	O	Si	Ni	Cr	Ta	Nb	Ti
ppm	10	14	4.3	200	417	30	100	100	4.26%	1.96%	Balance
0.2% Proof strength			-	256 MPa (Longitudinal); 334 MPa (Transverse)							
Ultimate Tensile Strength (UTS)			-	418 MPa (Longitudinal & Transverse)							
%Elongation (L_o = 50 mm)			-	37 (Longitudinal); 33 (Transverse)							

Microchemical characterization across the weld interface was carried out using Cameca SX50 electron probe micro analyzer (EPMA). Accelerating voltage of 20 kV and beam current of 20 nA was used for the analysis. X-ray generation volume was restricted to 1 μm. Details of analyzing crystal and X-ray reflection line used to quantify the elements are given in Table 3. Quantitative analysis was performed by comparing the intensities of Kμ or Lμ radiation of the elements obtained from the sample with that of the standards. Obtained X-ray intensities were corrected for atomic number, absorption and fluorescence effects to obtain corresponding accurate chemical concentration.

RESULTS AND DISCUSSION

Characterization of 'as received' explosive joints

Fig. 1 shows the optical microstructure and superimposed hardness profile of 'as received' explosive welded joint. A sharp interface was observed between TiTaNb and SS with no observable change in the microstructure near the interface. The interface profile was found to be wavy indicating satisfactory welding between the dissimilar alloy systems. In explosive welding, the impact velocity and collision angle are adjusted for the alloy systems to determine the impact welding domain which consists of the wavy interface, smooth interface and the transition zone [7]. In this welding domain, a wavy interface is preferred since it increases the bond area, produces greater depth of shock hardening thereby rendering stronger joints, and also isolates trapped melts as islands at the crests and troughs of the waves [8]. In addition, other characteristic features of any explosive welded joint [9] like shrinkage cavities and solidified melt zones were also observed at the interface of TiTaNb and SS. Micro-hardness profile showed maximum hardness of around 425 VHN near the interface on SS side. An overall increase in hardness (SS- 375 VHN and TiTaNb-225 VHN) was observed on both sides of the weld joint compared to the starting material (SS μ 230 VHN and TiTaNb-200 VHN). Increase in hardness very near to the interface may be a result of severe plastic deformation undergone by the base plate during explosive cladding [8]. To understand the overall increase in hardness, the base material micro-structures were examined more closely. Fig.2(a) and Fig.2(b) show the optical microstructures corresponding to 304L SS and TiTaNb respectively. Austenitic stainless steel showed a severely deformed microstructure with deformation twins and shear bands. Plastic deformation due to the passage of shock waves has resulted in a microstructure full of defects contributing to hardness increase in the material. Ti-5Ta-1.8Nb which showed only marginal increase in hardness had grains elongated in the welding direction. Similar observations on the microstructure and hardness have been reported in explosive weldments of similar (steels) [10] and dissimilar (cp-titanium/stainless steel) systems [11].

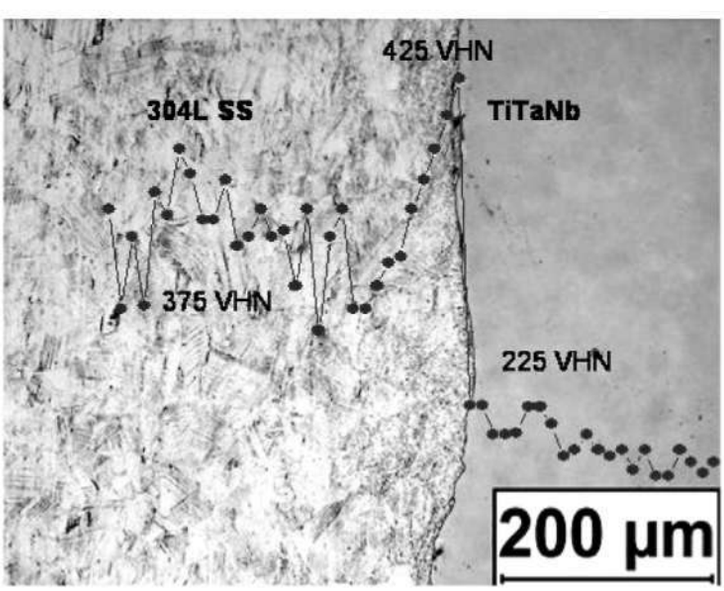

Fig. 1 : Optical microstructure and superimposed hardness profile of 'as received' explosive joints

X-ray diffraction pattern obtained from 304L SS (Fig. 3(a)) showed the presence of bcc phase in addition to the expected fcc phase. (110) and (211) peaks corresponding to the μ phase were obtained in addition to (111) and (220) peaks corresponding to the μ phase. From the relative intensities of μ ?and μ peaks, bcc phase was found to be the predominant phase in SS 304L after explosive cladding. It has been reported in literature that 304 stainless steel which has a metastable austenite matrix is susceptible for strain induced martensitic transformation [12]. Formation of martensite was extensively studied as a function of strain rate and its volume

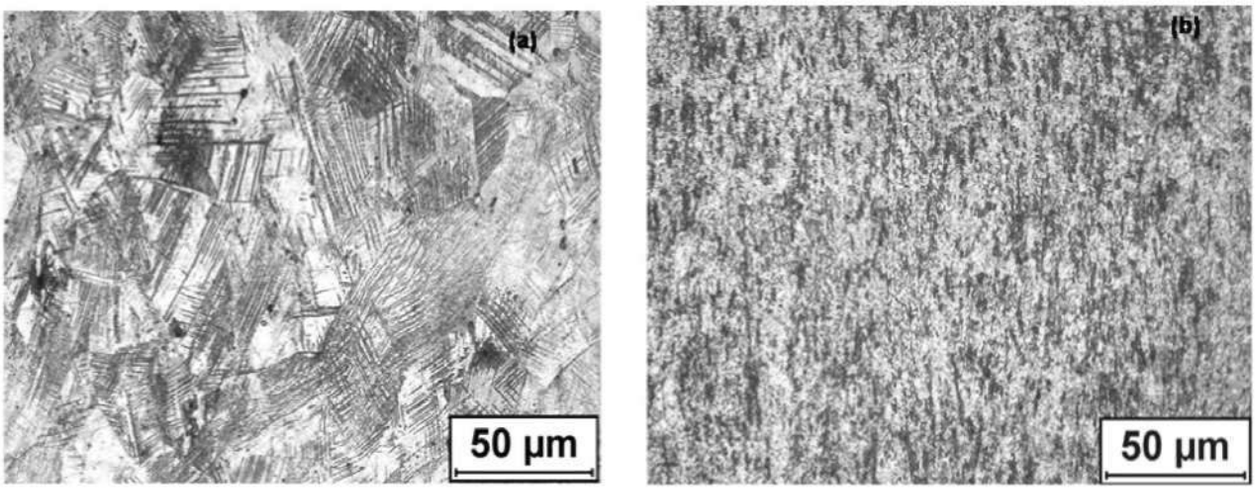

Fig.2 Optical micrographs showing (a) deformation twins and shear bands in 304L SS and (b) grains elongated in the direction of welding in Ti-5Ta-1.8Nb alloy

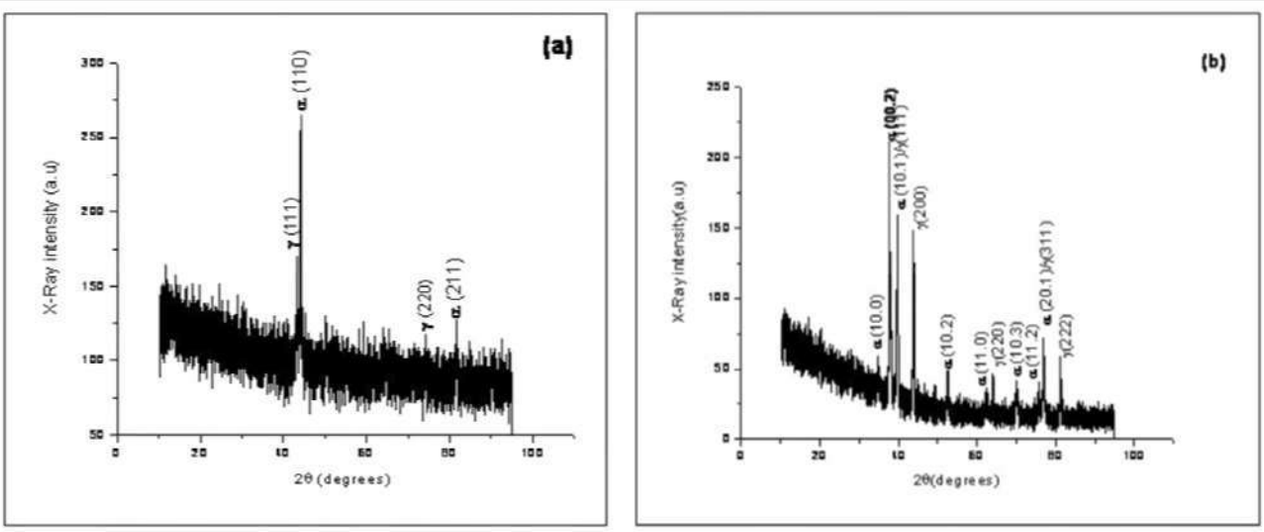

Fig. 3 XRD patterns showing the presence of (a) bcc phase in addition to fcc phase in 304L SS and (b) metastable fcc phase in TiTaNb alloy

fraction was related to the percentage of deformation [13]. Similarly on TiTaNb side, in addition to the peaks corresponding to hcp µ phase, additional peaks corresponding to fcc µ2phase were also obtained (Fig. 3(b)) which is rather surprising since orthorhombic ¾µ" phase only was expected after deformation in Ti alloys [14]. Since the XRD patterns were obtained from TiTaNb overlay plate well away from the interface, the authors are convinced that this observation of additional peaks identified as 'µ' was indeed from the flier plate only, and not because of the presence of intermetallic phases. Even though the formation of metastable fcc phase of Ti is well documented in Ti based thin films [15], not much information is available in literature on bulk alloys except for a recent report on metastable fcc phase formation in high pressure exposed (100 GPa) Ti-Mg based alloys [16]. In addition, an indication of texturing was also noticed on TiTaNb side with the peak intensity from (002) plane dominating when compared to (101) plane. This observation, however, requires further confirmation. XRD patterns obtained from the interface (Fig. 4) did not show the presence of intermetallic phases. Only peaks corresponding to the matrix phases were present.

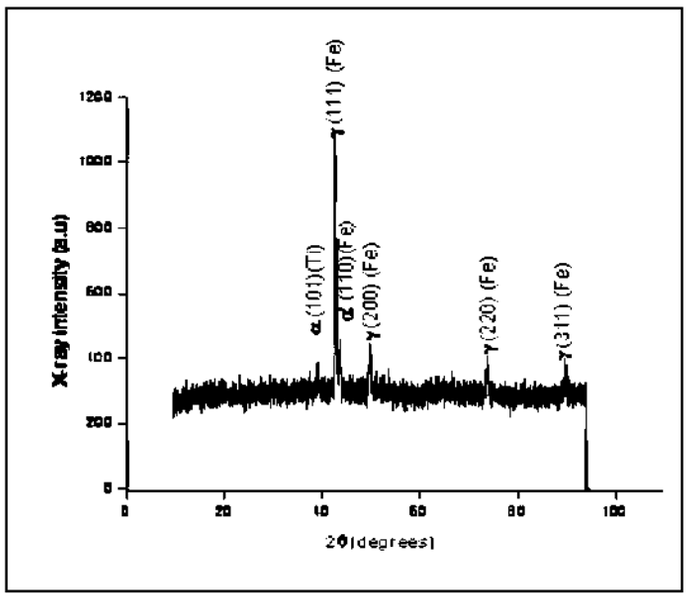

Fig. 4 XRD pattern obtained from the interface of explosive welds

Elemental redistribution profiles obtained using electron microprobe for Fe, Ti (Fig. 5(a)), Ta, Nb (Fig. 5(b)) and Cr, Ni (Fig. 5(c)) showed sharp transition in the concentration profiles near the interface. No evidence could be obtained for the existence of intermetallic phases within the resolution limit of EPMA. In direct fusion welded joints, due to inter-diffusion of alloying elements intermetallic phases will form as separate zones parallel to the interface. However, in the case of explosive weldments such zone formations are not expected since diffusion of alloying elements was avoided. However, intermetallic phases may be present as isolated pockets near the solidified melt zones which form due

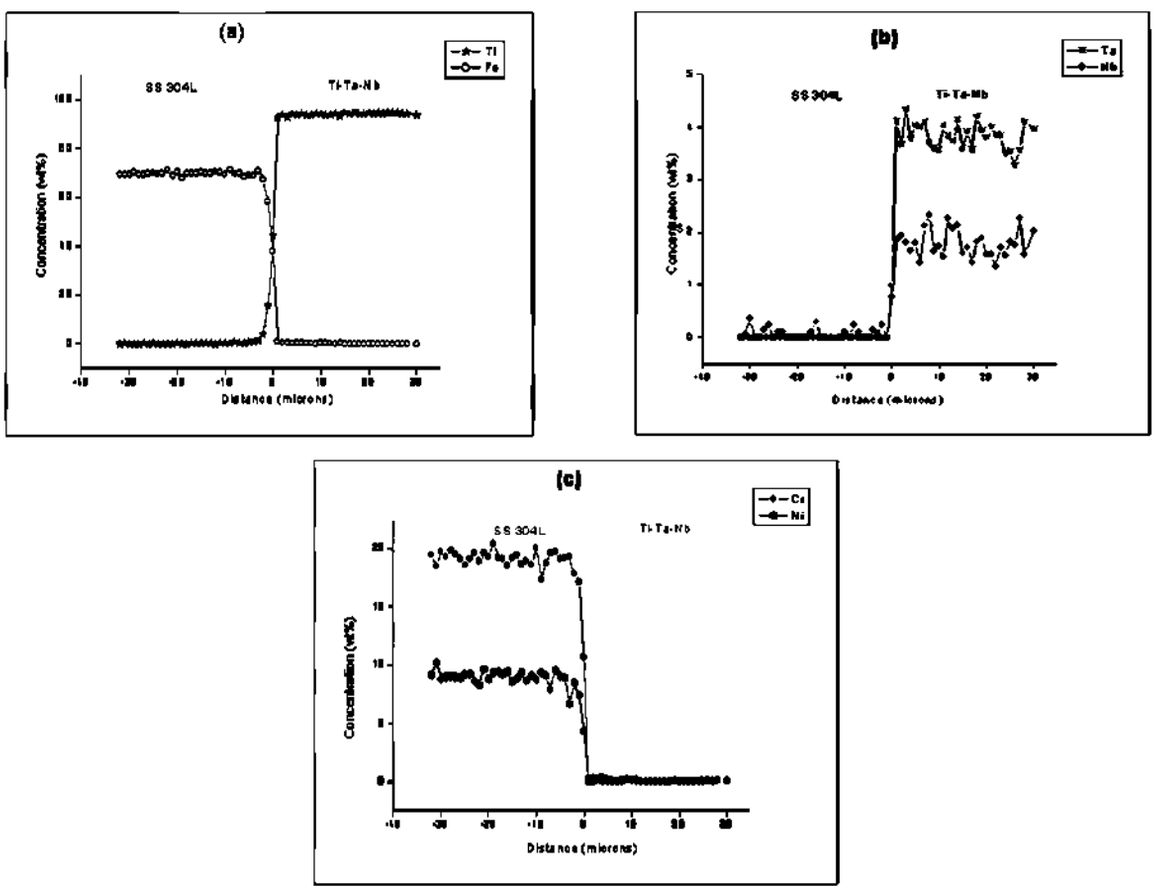

Fig. 5 Elemental redistribution profiles for (a) Fe, Ti (b) Ta, Nb and (c) Cr, Ni showing sharp change in concentration across the interface of 'as received' explosive clad

to jetting of the molten metals during the welding process. If the volume fraction and size of such isolated packets is less it is possible that neither EPMA nor XRD detect their presence. Hence, characterization using transmission electron microscope (TEM) is in progress for further confirmation.

Characterization of explosive joints after heat treatment

Presence of highly deformed microstructure very near the interface on SS 304L side in 'as received' explosive joints may affect the performance of the joint in actual service condition. Hence, it is essential to heat treat the explosive joints before service or further fabrication procedures. Fig. 6(a) to Fig. 6(e) show the secondary electron images of welds heat treated at 873 K for 1, 2, 5, 10 and 20 h respectively. No observable microstructural change could be seen at the interface except for the formation of a dark zone for longer durations of exposure at 873 K (shown by arrow mark in Fig. 6(e)) and formation of porosities parallel to the interface on SS side which increase in volume fraction with duration of exposure. EPMA elemental concentration profiles obtained for Fe, Ti, Ni, Cr, Ta and Nb (Fig. 7) for 873 K-1h heat treated joints showed limited diffusion up to a distance of 1-2 μm. Due to limited mutual solubility of Fe and Ti (maximum

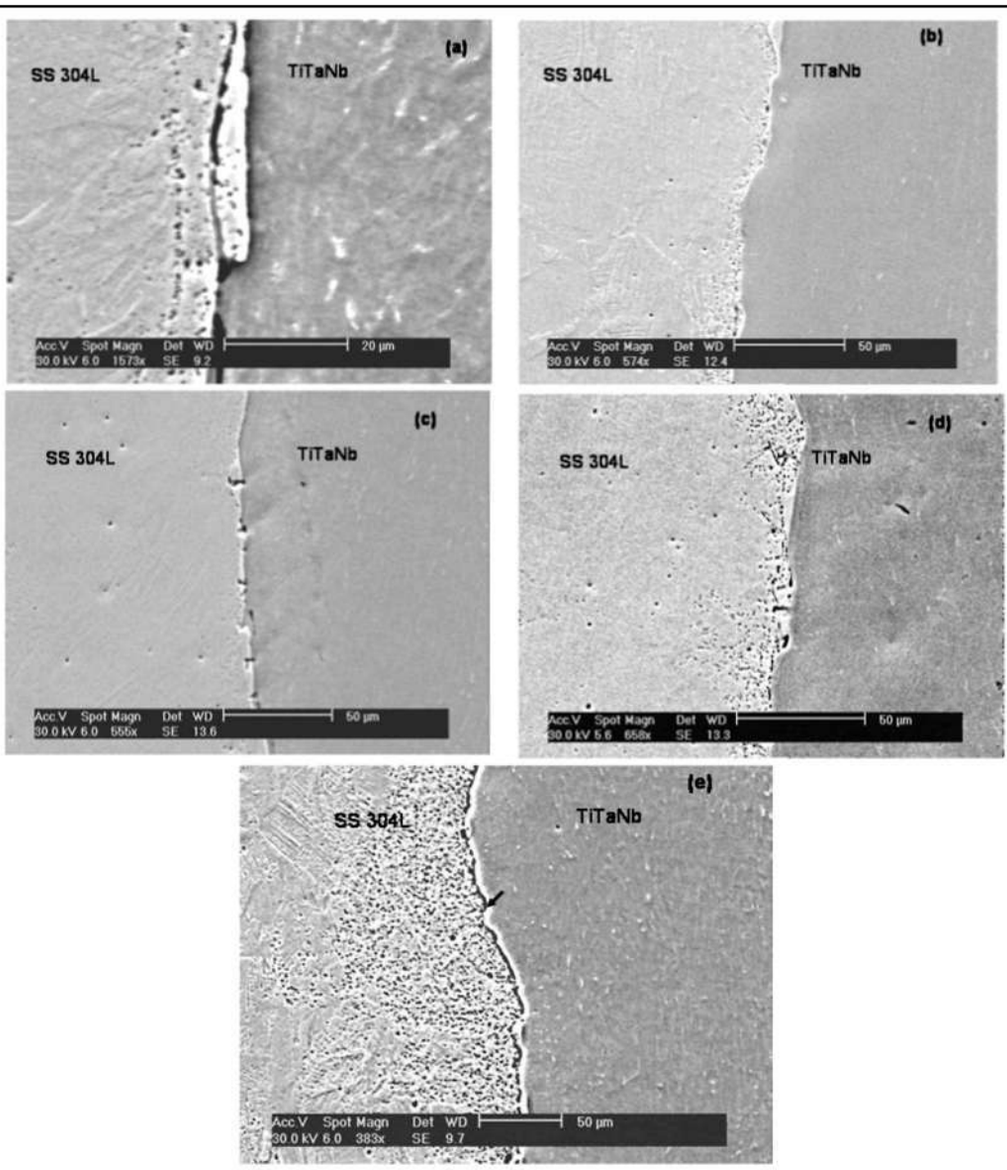

Fig. 6 Secondary electron images showing the microstructure at the interface of 873 K heat treated explosive joints for (a) 1 (b) 2 (c) 5 (d) 10 and (e) 20 h

solubility of Fe in μ Ti is 0.05 % at 973 K and for Ti in μ-Fe is 0.8 % at 1423 K) it is possible that inter-diffusion leads to the formation of intermetallic phases at the interface. EPMA profiles (Fig.7) showed smoothly varying concentration profiles with no steps corresponding to the dark zone (arrow marked in Fig. 6(e)) for both Fe and Ti indicating that the width of the intermetallic zone may be less than the resolution limit of EPMA. It was also observed that Fe diffusion in Ti which has an hcp structure was faster than the diffusion of Ti in Fe having a packed fcc lattice structure. In the thermodynamic assessment of Fe-Ti system [17], it has been reported that diffusivity of Fe in μ -Ti is in the range of 10^{-14}-10^{-11} m^2/s at temperatures from 1173 to 1373 K compared to the diffusivity of Ti in μ-Fe which ranges from 10^{-18}-10^{-14} m^2/s at temperatures from 1223 to 1473 K. The porosities observed in Fig. 6 also may be the 'Kirkendall porosities' forming due to the unequal diffusion rates of Fe and Ti. It has been reported that the unequal flux of elements across the interface will be balanced by a corresponding flux of vacancies [18] which form preferably in the alloy having lower melting point. These vacancies may condense to form voids which increase in volume fraction as a function of time of heat treatment. Initially porosities were observed only close to the interface on SS side which has the lower melting point. As the duration of heat treatment was increased, the volume fraction and the width of the porous region also increased which is in accordance with the observation made in literature [18].

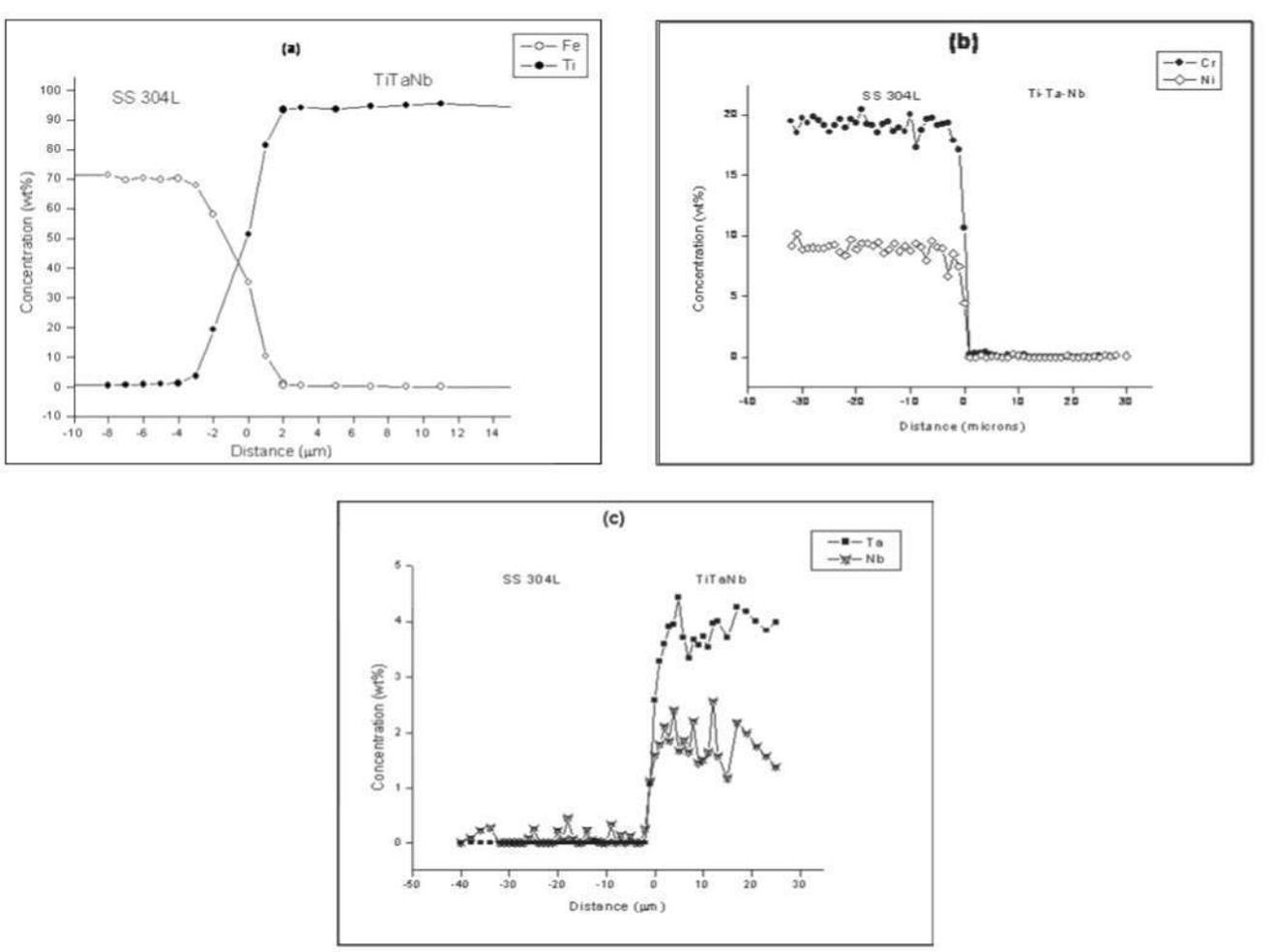

Fig. 7 : EPMA elemental concentration profiles for (a) Fe, Ti (b) Cr, Ni and (c) Ta, Nb for welds heat treated at 873 K for 1h

After 20 h of exposure at 873 K, there was only a marginal increase (~ 3 µm) in the diffusing distance (Fig. 8) probably because of the slower diffusion kinetics. XRD patterns gave evidence for the presence of FeTi, Fe_2Ti type of intermetallic phases in addition to titanium oxide (TiO) in both 1 h (Fig. 9(a)) and 20 h (Fig. 9(b)) heat treated welds. The intensities corresponding to the intermetallic phases increased with the duration of exposure.

Increasing the heat treatment temperature to 1073 K brought about considerable changes in the interface microstructure. Even a 1 h heat treatment showed formation of different zones at the interface as seen in the back scattered electron (BSE) image in Fig. 10(a). Fig. 10(b) shows the BSE image for 20 h heat treated weld where at low magnification, five zones are clearly visible. When the magnification was further increased, it was found that zone 2 itself can be further subdivided into four zones namely 2a, 2b, 2c and 2d. Number and width of zones increased with the time of heat treatment.

Elemental concentration profiles obtained using EPMA for 1 and 20 h heat treated specimens are given as Fig. 11(a) and (b) respectively. The diffusing distances were found to increase with the duration of heat treatment. Fe diffusion into Ti was found to be faster than Ti diffusion into Fe. From Fig. 11(b), it can be seen that there are number of steps in the concentration

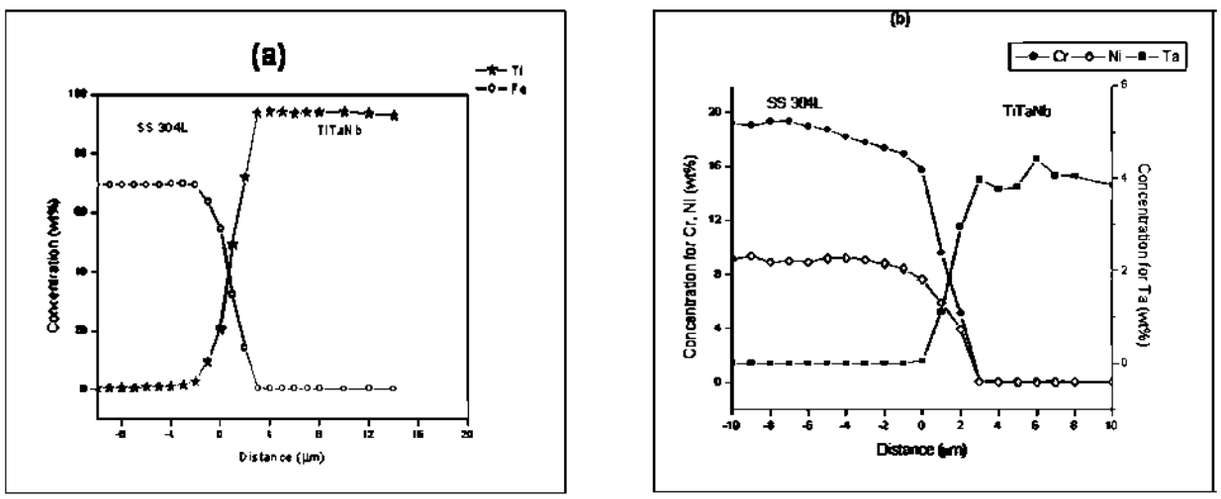

Fig. 8 EPMA elemental concentration profiles for (a) Fe, Ti (b) Cr, Ni and Ta for welds heat treated at 873 K for 20 h

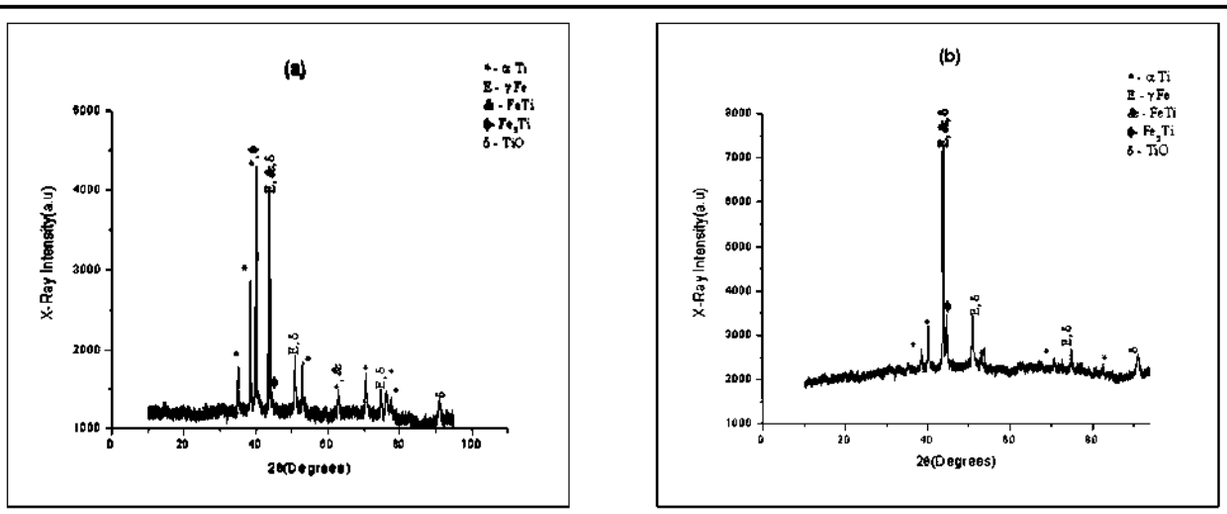

Fig. 9 X-ray diffraction profiles obtained from 873 K heat treated joints for (a) 1h and (b) 20h

profile corresponding to the formation of different phases. For all durations of heat treatment, enrichment of Cr was observed very near the interface on SS side. It has been reported that [5] diffusion of Ti to SS side decreases the activity of Cr near the interface without changing its concentration gradient. This leads to an 'uphill' diffusion of Cr within SS resulting in the formation of μ phase. EPMA concentration profile did not indicate the formation of phase (Cr in the range of 43 – 46 wt% having very low solubility for Ti, probably because width of the phase may be less than the resolution limit of EPMA.

X-ray diffraction patterns obtained from 1073 K 1h (Fig. 12(a)) and 20h (Fig. 12(b)) heat treated welds also confirmed the formation of intermetallic phases like FeTi, Fe_2Ti along with titanium oxide (TiO). The peak intensity for μ-Ti phase was enhanced compared to 'as received' welds due to the stabilization of μ phase near the interface which is a result of diffusion of Fe from the SS side. Similarly, there were peaks corresponding to μ phase also, but due to the presence of other overlapping peaks, an independent peak corresponding to the μ phase was not present.

After comparing the concentration of major alloying elements like Fe, Cr and Ti with the isothermal section of Cr-Fe-Ti ternary phase diagram at 1073 K, it was concluded that the following phases form as a function of distance starting from the SS side:

$$\underset{zone\ 1}{\gamma(Fe)} \rightarrow \underset{zone\ 2a}{\gamma(Fe)+\chi} \rightarrow \underset{zone\ 2b}{\gamma(Fe)+\chi+\lambda} \rightarrow \underset{zone\ 2c}{\lambda+FeTi} \rightarrow$$

$$\underset{zone\ 2d}{\lambda+FeTi+\beta(Ti)} \rightarrow \underset{zone\ 3}{FeTi+\beta(Ti)} \rightarrow \underset{zone\ 4}{\beta(Ti)} \rightarrow \underset{zone\ 5}{(\alpha+\beta)Ti}$$

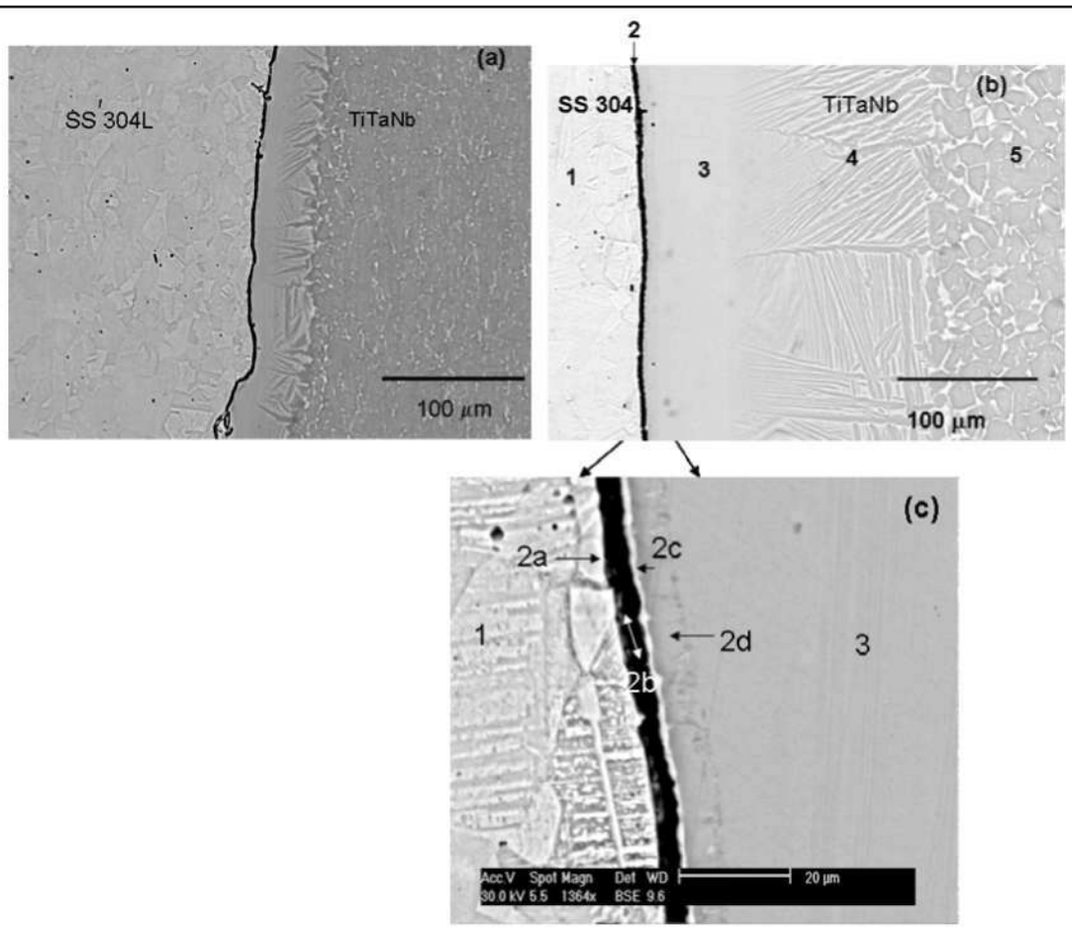

Fig. 10 BSE images of 1073 K heat treated specimen for (a) 1h (b) 20h and (c) image taken at high magnification showing various zones in zone 2

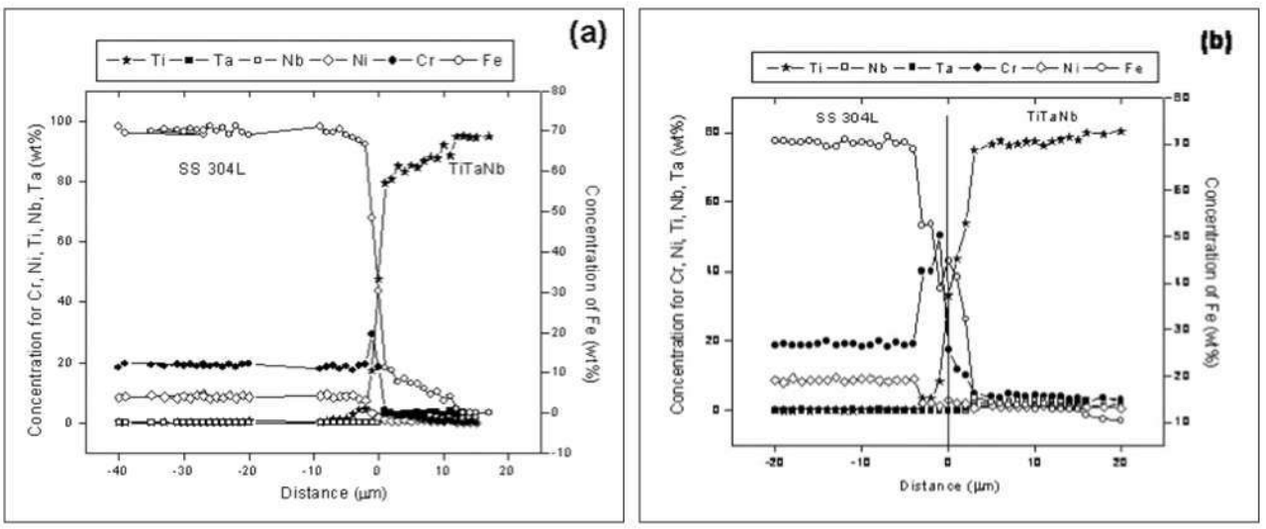

Fig. 11 Elemental concentration profiles obtained using electron microprobe for 1073 K-20 h heat treated specimen

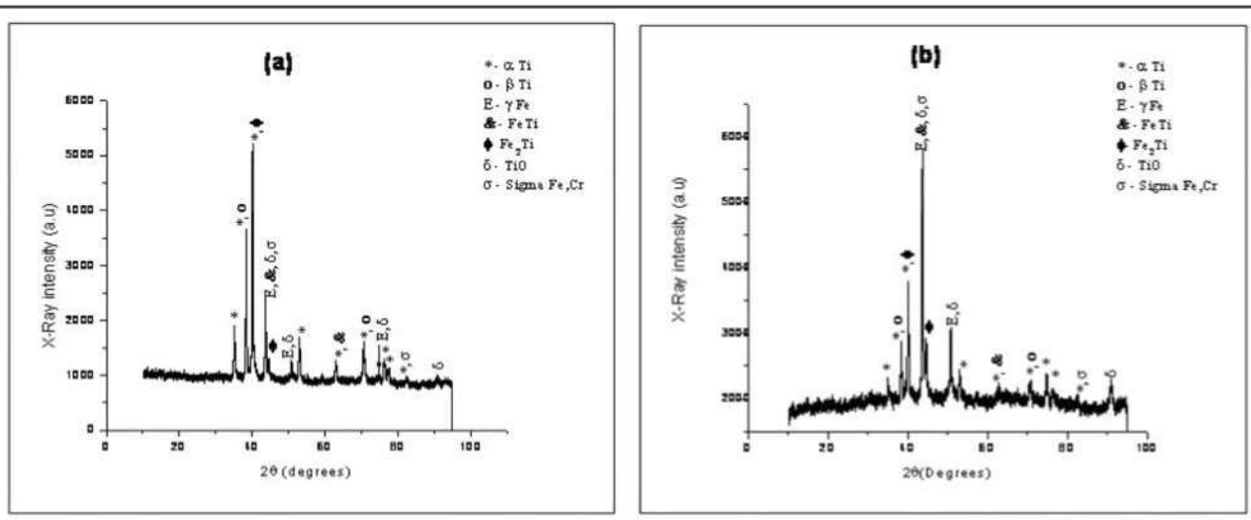

Fig. 12 XRD patterns confirming the formation of intermetallic phases in 1073 K heat treated welds for (a) 1h and (b) 20h

Apart from the base materials, in total, six zones were found near the interface. Elemental X-ray mapping given as Fig. 13 clearly showed enrichment of Cr in zone 2a (Fig. 10(c)) corresponding to the formation of μ phase which has a composition range of 19-34 % Cr, 49-69 % of Fe and maximum up to ~ 17 % of Ti. Similarly, zone 2c which consists of Fe and Ti based intermetallic phases (& (Fe_2Ti) + FeTi) was also clearly revealed in Fig. 13 showing simultaneous enrichment for Fe and Ti. In addition, Ni and Ta also showed enrich-ment in zone 2c. Crosschecking with isothermal section of Fe-Ni-Ti ternary phase diagram at 1173 K, it was found that & phase has considerable solubility for Ni, maximum up to 20 % [19]. In addition, it was found that in the ordered (Fe,Ni)Ti phase Fe and Ni have complete solubility which explains for the enrichment for Ni observed in zone 2c. Similarly Ta also may be having solubility in FeTi phase which has to be checked with Fe-Ti-Ta ternary phase diagram. Zone 2b having three phase equilibrium was not having enhanced contrast in Fig. 13 probably because of higher contrast on both sides corresponding to Cr and Fe enrichment.

With the observations made with the help of X-ray imaging and elemental concentration profiles the micrograph given as Fig. 10(b) can be re-looked to relate the phase formation to observed morphology. Zone 1 corresponds to the

original SS 304L base material, zone 2 consists of all the intermetallic phases along with the original interface, zone 3 has a two phase structure, i.e μTi + FeTi, zone 4 is predicted to be μTi phase and zone 5 microstructure corresponds to original μ-μ Ti alloy. In zone 3, the high temperature bcc μ phase was stabilized due to the presence of considerable amount of beta stabilizers like Fe (~ 10 wt%) and Cr (~ 2 wt%). However, in zone 4, the amount of μ stabilizers available was not enough to retain the μ phase at room temperature and it transforms to Widmanstatten μ-μ structure consisting of bright μ phase embedded in μ Ti during cooling. Simultaneous enrichment of Fe and Ta in the bright regions of zone 4 (Fig. 14) further confirmed the formation of acicular μ phase. In zone 5, μ phase transforms to equiaxed μ-μ structure. It has been reported [5] that existence of thick μ-Ti phase at the interface as well as the formation of Fe and Ti rich intermetallic phases near the interface will have significant effect on the performance of the weld in actual service conditions. From the above studies, it was inferred that width of zone 2 which consists of intermetallic phases along with the original interface will be deciding the bond strength of the explosive joints.

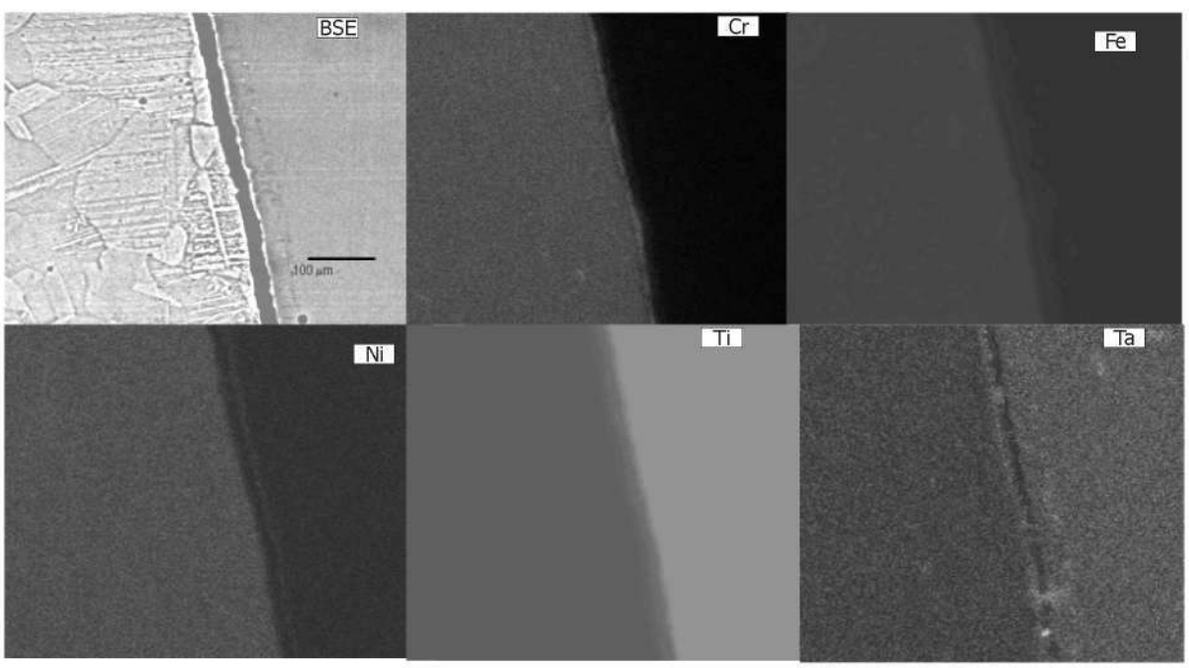

Fig. 13 BSE image and elemental X-ray images showing the enrichment of Cr in zone 2a and simultaneous enrichment of Fe, Ti, Ni and Ta in zone 2c

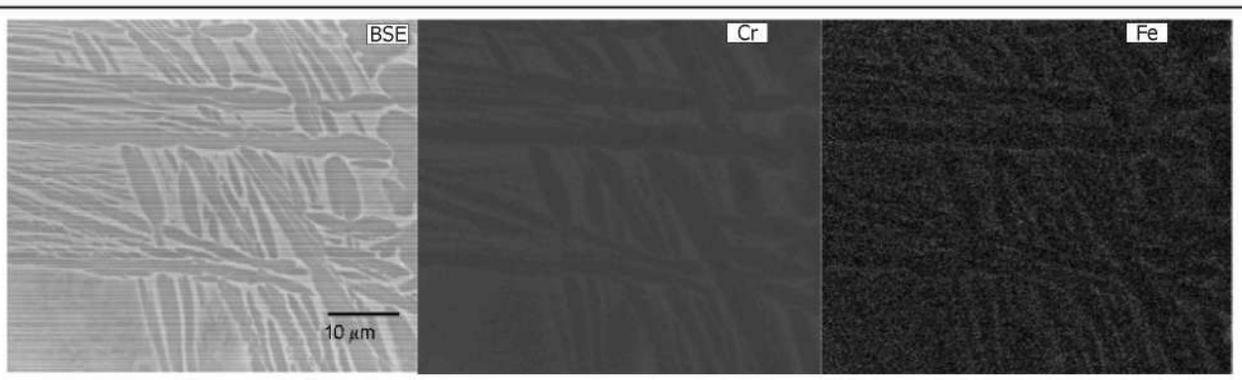

Fig. 14 BSE image and elemental X-ray images showing simultaneous enrichment of Fe and Ta in the bright regions of zone 4

CONCLUSIONS

- Ti-5Ta-1.8Nb and 304L austenitic stainless steel were joined by explosive welding process. From electron microprobe and X-ray diffraction based analysis, intermetallic phases were found to be absent in 'as received' explosive joints.
- Both Ti-5Ta-1.8Nb and 304L SS base plates were found to exhibit deformation induced phase transformation after explosive welding.
- Increase in heat treatment temperature enhanced diffusion of major alloying elements. Diffusing distances for Fe, Cr in TiTaNb was more than that of Ti in SS. Diffusion of Fe and Cr to TiTaNb side stabilized the high temperature μ-Ti phase.
- Intermetallic phases like FeTi and Fe_2Ti were detected at the interface for all processing temperatures. Width and number of interaction layers increased as a function of processing temperature and time.
- It was inferred that explosive welds have to be stress relieved at temperatures less than 873 K subsequent to welding.

ACKNOWLEDGEMENT

The authors thank Dr. Baldev Raj, Director IGCAR and Dr. T. Jayakumar, Director MMG for their encouragement and support throughout the period of this project. The authors also thank Dr. S. Murugesan for his useful suggestions with respect to X-ray diffraction analysis.

REFERENCES

1. Kamachi M U, Ananda R B M, Shanmugam K, Natarajan R and Baldev R (2003). Corrosion and microstructural aspects of dissimilar joints of titanium and type 304L stainless steel, J. Nucl. Mater., 321, 40-48.
2. Pocalyko A (1987). Fabrication of explosion-welded titanium-clad composites, Welding Journal, 25, 24-30.
3. Pocalyko A (1965). Explosion clad plate for corrosion service, Mater. Protection, 4(6), 10-15.
4. Akbari M S A A and Farhadi S P (2009). Experimental investigation of explosive welding of cp-titanium /AISI 304 stainless steel, Mater. and Design, 30, 459-468.
5. Akbari M S A A and Farhadi S P (2008). Effect of post-weld heat treatment on the interface microstructure of explosively welded titanium-stainless steel composite, Mater. Sci. Engg., A494, 329-336.
6. Changoing X and Zhanpeng J (1990). On the evolution of microstructure and diffusion paths in the titanium-steel explosion weld interface during heat treatment, J. Less Common Metals, 162, 315-322.
7. Jaramillo D, Szecket A and Inal O T (1987). On the transition from a waveless to a wavy interface in explosive welding, Mater. Sci and Engg., 91, 217-222.
8. Akbari M S A A, Al-Hassani S T S and Atkins A G (2008). Bond strength of explosively welded specimens, Mater. and Design, 29, 1334-1352.
9. Tamhankar R V and Ramesam J (1974). Metallography of explosive welds, Mater. Sci and Engg., 13, 245-254
10. Acarer M, Gulenc B and Findik F (2003). Investigation of explosive welding parameters and their effects on microhardness and shear strength, Mater. and Design, 24, 659-664
11. Kahraman N, Gulenc B and Findik F (2005). Joining of titanium/stainless steel by explosive welding and effect on interface, J. Mater. Proc. Technol., 169, 127-133.
12. Roberti Da, Rocha M and Silva de O C A (2009). Evaluation of the martensitic transformation in austenitic stainless steel, Mater. Sci and Engg., A517, 281-285
13. Das A and Tarafder S (2009). Experimental investigation on martensitic transformation and fracture morphologies of austenitic stainless steel, Inter. J. Plasticity, In Press.
14. Wang L, Lu W, Qin J, Zhang F and Zhang D (2009). Influence of cold deformation on martensitic transformation and mechanical properties of Ti-Nb-Ta-Zr, J. Alloys and Comp., 469, 512-518.
15. Lai J B, Chen L J and Liu C S (1999). Ion beam induced formation of metastable fcc-Ti phase in epitaxial Ti/Cu (111) Si structures, Micron, 30(3), 205-211
16. Phasha A J, Kasonde H and Ngoepe P E (2008). Effect of pressure on the metastable phase formation of equilibrium immiscible Ti-Mg system studied by ab-initio technique and mechanical milling. http://researchspace.csir.co.za/dspace/bitstream/.../1/Phasha_P_2008.pdf
17. Cacciamani G, De Keyzer J, Ferro R, Klotz U E, Lacaze J and Wollants P (2006). Critical evaluation of the Fe-Ni, Fe-Ti and Fe-Ni-Ti alloy systems, Intermetallics, 14, 1312-1325
18. Kheder A R I and Greenwood G W (1993). Some characteristics of porosity arising because of the Kirkendall effect, Defect and Diffusion Forum, 95-98, 573-578
19. Riani P, Cacciamani G, Thebaut Y and Lacaze J (2006). Phase equilibria and phase transformation in the Ti rich corner of the Fe-Ni-Ti system, Intermetallics, 14, 1226-1230.